

Enhancement the efficiency of FRP External strengthening system of RC Flexural Member

Azza.Abdelrashed¹, T.Aly², W. Ibrahim³, M. Mege⁴

^{1, 2, 3, 4} University of Helwan – Egypt.

Abstract: This paper presents an experimental study on twelve reinforced concrete (RC) slabs strengthened with carbon, glass, basalt fiber reinforce polymer (CFRP) laminate/sheet under four-point bending, aiming to reveal the effects of the bond-dependent coefficient, (K_m) on the load-carrying capacity of strengthened the slabs at debonding failure (i.e. debonding strength). For the purpose, the test specimens are such designed to explore effects of several important factors, including modulus of elasticity of the fibers, the thickness of the used fibers, and the number of layers. The experimental results showed that the number of plies and thickness of the carbon laminate/sheet are strongly influences the debonding strengths of the strengthened slabs. It was also found that the ($A_{\text{fiber}}/A_{\text{steel}}$) ratio is major parameter that affects the performance of strengthened slabs.

Keywords: FRP, debonding, concrete, slabs, strengthening.

1. INTRODUCTION

One of the successful structural applications of fiber reinforced polymers (FRP) is the external composite strengthening for repair and upgrade of the structural capacity and ductility of concrete members. The advantages of FRP composites are high strength, low weight, good corrosion resistance and ease of installation. Existing studies have showed that debonding failure is a typical failure for concrete beams strengthened with externally bonded FRP composites. The ACI-440 guidelines recommended the required cross-sectional area of FRP fabrics is based on satisfying a limited effective strain in the fibers matching a predetermined value controlled by the bond-dependent coefficient, (K_m). The bond-dependent coefficient is account only for stiffness of the laminate/sheet and ignores the stiffness of the member to which the laminate is bonded. The objective of this paper is to estimation the bond-dependent coefficient, taking into account the modulus of elasticity of the fibers, the thickness of the used fabrics, compressive strength of concrete, and the number of layers. Failure modes have been observed in the experimental program. These modes can be divided into two categories: "FRP debonding" and "FRP fracture" failures (Buyukozturk, 2004). Since in many cases, the failure of strengthened beams is governed by the FRP debonding failure, the investigation of the stresses at the concrete/strengthening layer interface is an important issue in analysis and design. An analytical model is presented in this paper to calculate the normal interfacial stress. The predicted capacities are compared to the measured values.

2. EXPERIMENTAL PROGRAM

2.1 Test specimens

Twelve simply supported RC slabs with a span of 2 m were constructed and tested at the Structural Laboratory of Helwan University. Details of the test specimens are given in Table 1. This paper focuses mainly on the analytical prediction and estimating of the bond-dependent coefficient, K_m . The top and bottom reinforcement were 10 mm diameter steel bars spaced at 150mm as shown in Fig. 1. All slabs were constructed with a depth of 150mm. four different types of strengthening schemes were used. Two slabs were strengthened using carbon laminates. Two slabs were strengthened using carbon sheets. Two slabs were strengthened using glass sheets. Twonormal compressive strength of concrete slabs were strengthened using basalt sheets, two high compressive strength of concrete slabs were strengthened using basalt sheets, and one slab was tested as control specimen at normal and high compressive strength. With the maximum moment occurring at the mid-span section of the slab, failure could be due to debonding, concrete crushing and rupture of the externally bonded laminates or sheets. The specimens were designed as per ACI 318-2002 design guideline (ACI 318, 2019).

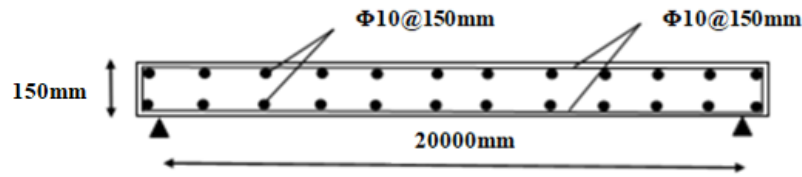


Figure 1: reinforcement details of slab specimens

2.2 Material Properties

- Reinforcing Steel: Based on testing three 10 mm diameter steel bars, the rebars have a yield strength of 560MPa with a modulus of elasticity of 200 GPa and an ultimate strength of 640MPa.
- Concrete: The concrete mix was prepared at the laboratory to provide a nominal strength of 25 MPa and high strength 60 MPa using Type-I- Portland cement. The maximum aggregate size was 20mm to ensure good workability of the concrete around the steel rebars and eliminate formation of any honey combing.
- Strengthening Sheets: The strengthening laminates and sheet used in the current study are illustrated in Fig. 2 and the mechanical properties are given in Table 2.
- Epoxy: The manufacturer (SIKA) provides the mechanical properties of the epoxy.



Figure 2: strengthening materials laminates and sheets used in the current study

Table 1: Specimens Details

slabs	Compressive strength	Tension steel	fiber				
		mm ²	Type	Number of layers	Thickness (mm)	Area Fiber mm ²	A _F /A _S
S1	Normal compressive strength F _{cu} =25MPa	560	N/A	N/A	N/A	N/A	N/A
S2		560	Carbon Sheet	1	0.165	33	0.109
S3		560	Carbon Sheet	2	0.165	66	0.212
S4		560	Glass Sheet	1	0.168	33.6	0.107
S5		560	Glass Sheet	2	0.168	67.2	0.214
S6		560	Basalt Sheet	1	0.28	56	0.18
S7		560	Basalt Sheet	2	0.28	112	0.36
S8		560	Carbon Laminate	1	1.2	60	0.19
S9		560	Carbon Laminate	2	1.2	120	0.38
S10	high compressive strength F _{cu} =60MPa	560	N/A	N/A	N/A	N/A	N/A
S11		560	Basalt Sheet	1	0.28	56	0.18
S12		560	Basalt Sheet	2	0.28	112	0.36

Table 2: Mechanical properties of strengthening materials

Material	Strength		Modulus of elasticity	Ultimate strain
	Type	MPa	GPa	
Concrete	Compressive strength	25	20	0.003
steel	Tensile strength	640	200	0.0028
	Yield strength	560		
Carbon laminate	Tensile strength	3100	165	0.0140
Carbon sheet	Tensile strength	3500	230	0.017
Glass sheet	Tensile strength	2500	77	0.0214
Basalt sheet	Tensile strength	2310	90	0.0267
Epoxy adhesive	Tensile strength	45	10	0.0045

2.3 Test Setup and Instrumentation

All slabs were tested using a four point bending configuration to develop a constant moment region. The span of all slabs was kept constant at 1800 mm. The test setup allowed a constant moment region 600 mm. The slabs were supported on a roller support at one end and a hinged support at the other. One hydraulic jack 500 KN capacity was used to apply the load on top of a rigid steel beam that equally distributes the load at both load points. The test setup is shown in Fig. 3. Test results are used in the following sections to develop an analytical approach to predict flexural and delamination failures.

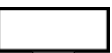
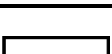
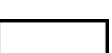
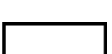
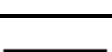


Fig. 3: Test setup

3. EXPERIMENTAL RESULTS AND ANALYSES

The failure modes of the test specimens, as well as yielding load and ultimate load, are reported in Table 3. As can be seen from Table 3, the strength and stiffness of the slabs are substantially increased. The ultimate load carrying capacity of the slabs increased by as much as 130% over their un-strengthened counterpart. The FRP debonding failure as observed in all the specimens. The $(A_{\text{fiber}} / A_{\text{steel}})$ ratio and number of layers are major parameters that affect the performance of strengthened slabs.

Table 3: Details of test specimens and experimental results

G.N	Slabs name	Prism cross section	Strengthening details	Layer numbers	A_{fiber}	Cracking load	Ultimate load	$\max@ \Delta$	FRP Strain ϵ_{fe} (exp)	steel, $\max \epsilon$ (10^{-6})
					mm^2	P_{cr} (KN)	P_{u} (KN)	ultimate load(mm)(Δu)		
Normal compressive strength	S1		Control slab	A/N	A/N	28	84	50	-	20962
	S2c1		Carbon sheet	1	33	29	95	33	0.0109	8443
	S3c2		Carbon sheet	2	66	36	102	25	0.0065	24881
	S4G1		Glass sheet	1	33.6	27	94	45	0.021	32191
	S5G2		Glass sheet	2	67.2	27	97	40	0.0112	39020
	S6B1		Basalt sheet	1	56	30	95	65	0.01309	42189
	S7B2		Basalt sheet	2	112	31	98	40	0.0086	39182
	S8Cstrip1		Carbon laminate	1	60	30	100	43	0.0095	25590
	S9Cstrip2		Carbon laminate	2	120	31	88	31	0.0048	2693
High compressive strength	S10		Control slab	A/N	N/A	35	85	40	-	25674
	S11B1		Glass sheet	1	56	37	96	46	0.015	42160
	S12B2		Glass sheet	2	112	40	107	50	0.00822	20123

3.1 The Development of Slab Deflection

The load-deflection at mid-span curves appear as four-stage as explained next. Before cracking, the curves are in elastic stage with the deflection increased with the increase of load. With the further increase of load, the cracks initiate in the slabs; as a result, the curves enter the second stage. At the late of the second stage, the tension bars yield signifying the beginning of the third stage during which the stiffness of slabs is further reduced. At the last stage, the curves begin to decrease after the occurrence of debonding failure. Fig. 4,5 shows the load-deflection curves of the strengthened slabs; the curve of the slab without strengthened is also shown in the figure for comparison.

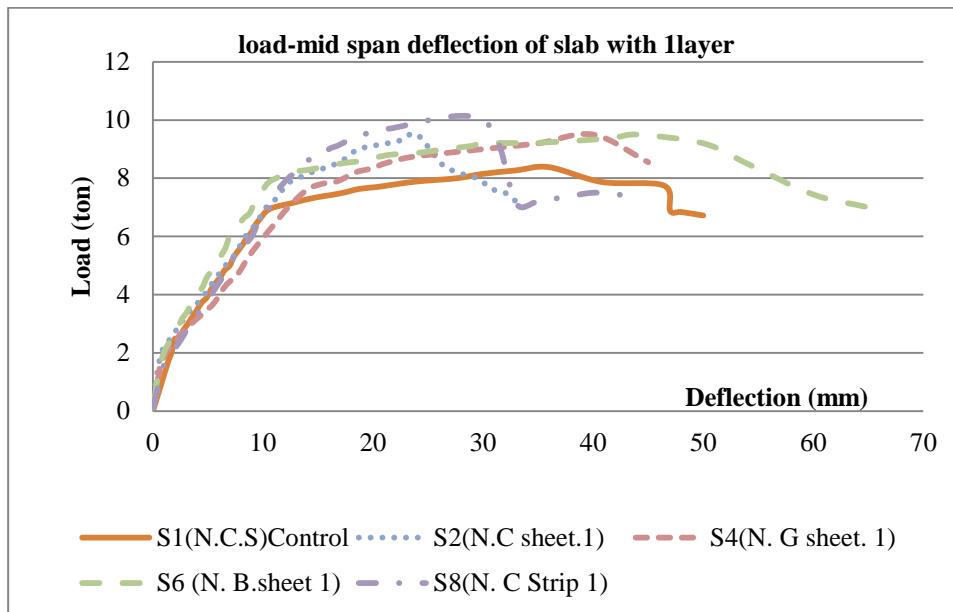


Figure 4: load-mid span deflection of slab with 1layer

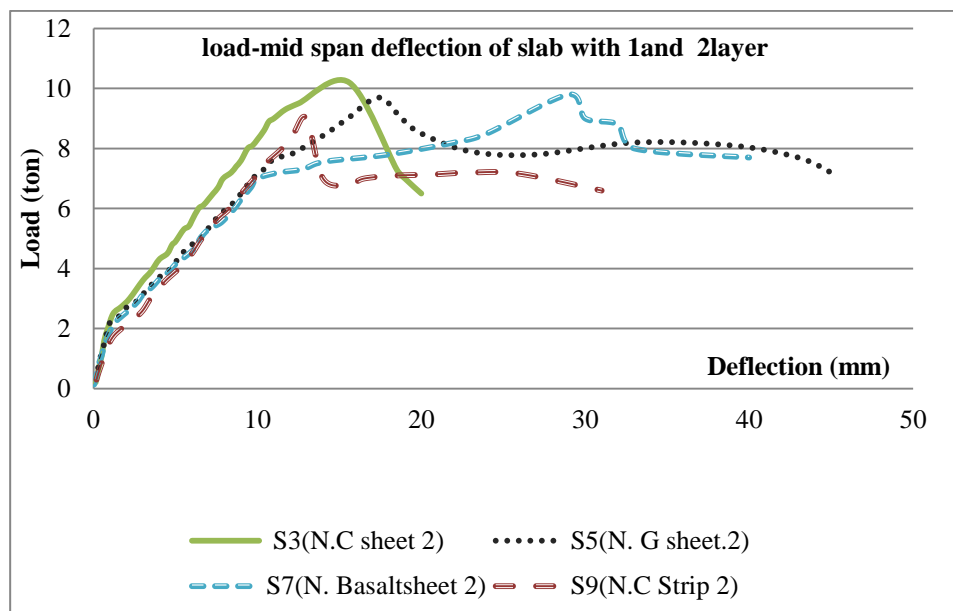


Figure 5: load-mid span deflection of slab with 2layer

3.2 Failure Process

The failure process can be divided into four stages as detailed next (Chen, 2006). (1) The elastic stage: this stage refers to the short stage during which only elastic deformation was measured and no cracking development was observed. (2) Crack initiation and development stage: with the increase of load, cracks were observed in the mid-span zone where the tensile stresses at bottom surface of slab are usually maximal. At the later period of this stage, most of cracks were stabilized and there was no new crack appearing in the bottom surface of slab. (3) Yielding stage: with the further increase of load, tension bars were yielded which was associated with a significant decrease of the slab stiffness. (4) Failure stage: all the slab specimens fail by FRP debonding or a combination of FRP debonding and FRP fracture, as shown in Fig. 5, As can be seen from Fig. 5, the FRP debonding failure normally initiates at the end of a critical crack under one of the loading points and propagates towards the debonded surface of FRP which is typical for FRP debonding failure (Hassan, 2002).



Fig. 5: The FRP debonding failure

4. THE ANALYTICAL METHOD TO PREDICT THE RESPONSE OF STRENGTHENED SLABS

This analytical method is based on the strain compatibility, equilibrium, and choice of material constitutive for concrete, reinforcing steel and FRP (ACI 440, 2000). A singly reinforced rectangular section is illustrated in Fig. 6 to develop an iterative analytical procedure to predict the structural response to load application. In the analysis, the following assumptions are made:

- Linear strain distribution throughout the full depth of the section;
- No slip between the longitudinal reinforcing steel and the surrounding concrete; No slip between the external FRP reinforcement and concrete substrate;
- No premature FRP separation or shear failure is accounted for;
- The tensile strength of the adhesive is ignored;
- No tensile strength is considered after cracking.

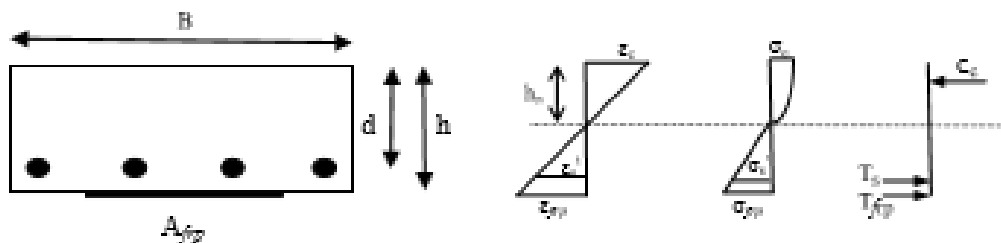


Fig. (6) Strain, Stress and Force distribution at section

To provide highly accurate prediction, concrete is assumed to follow the widely-used stress-strain curve by (ACI, 2002), reinforcing steel is modeled by elastic perfectly plastic curve in tension and compression, and FRP materials are assumed to behave linear elastically until to failure. Based on the strain compatibility and equilibrium of internal forces, FRP stress or external load can be predicted or a specific loading stage. Fig. 6 shows the strain, stress and force distribution along the depth of cross-section. In view of nonlinear behavior of concrete and reinforcing steel, this analysis should be performed by an iterative procedure. Every possible case should be checked for a given load or FRP stress at a certain section, such as whether the strain in the extreme fiber of concrete in compression is larger than ϵ_0 or not, compression steel or tension steel yields or not. In the analysis, the ultimate compressive strain of concrete ϵ_{cmax} is assumed to be 0.003. With respect to calculation of external load for a given FRP stress, it can be very easily preformed as follows: firstly assume $\epsilon_c < \epsilon_0$, calculate the neutral axis h_n and check whether the assumed conditions is met, if not, then assume $\epsilon_c < \epsilon_0$ and repeat the same procedure until the calculation result agrees with the assumption condition; secondly, the location of the resultant of compressive force can be easily determined on the basis of the calculated neutral axis; and finally, the external load can be determined by the equilibrium of the moment at given section. Determination of FRP stress is an inverse operation to the above stated and uses an iterative procedure following Fig. 6. The following is observed the steps to determines the load capacity and bond-debondentcoefficient.

Determined the load capacity

ACI (440.2R.2017)

$$M_n = [A_s f_s \left(d - \frac{\beta_1 c}{2}\right) + \psi X_f A_f f_f \left(d_f - \frac{\beta_1 c}{2}\right)]$$

$$P = M \times 2 / 0.6 \text{ (KN)}$$

Determined and enhancement the bond-debonding factor

: Determine the bond - dependent coefficient of the FRP system from ACI guide.

K_m = bond-dependent coefficient for flexure.

$$k_m(ACI) = \begin{cases} \frac{1}{60\epsilon_{fu}} \left(1 - \frac{nE_f t_f}{360,000}\right) \leq 0.90 \text{ for } nE_f t_f \leq 180,000 \\ \frac{1}{60\epsilon_{fu}} \left(\frac{90,000}{nE_f t_f}\right) \leq 0.90 \text{ for } nE_f t_f > 180,000 \end{cases} \quad (5.8)$$

: Enhancement the Determine of bond - dependent coefficient

$$k_m(Inhancing) = \begin{cases} \frac{1}{60m\epsilon_{fu}} \left(1 - \frac{nE_f t_f}{360,000}\right) \leq 0.90 \text{ for } nE_f t_f \leq 180,000 \\ \frac{1}{60\epsilon_{fu}} \left(\frac{90,000}{nE_f t_f}\right) \leq 0.90 \text{ for } nE_f t_f > 180,000 \end{cases}$$

*where n - number frp in 1 layer
 where m - number of layers*

: Determine the bond - dependent coefficient from Experimental test

From two equation

$$\epsilon_{fd} = 0.41 \sqrt{\frac{f'_c}{n E_f t_f}} \leq 0.9\epsilon_{fu} \text{ when } \epsilon_{fd} = 0.9\epsilon_{fu}$$

$$\epsilon_{fe} = \epsilon_{cu} \left(\frac{d_f - c}{c}\right) - \epsilon_{bi} \leq k_m \epsilon_{fd} \text{ when } \epsilon_{fe} = k_m \epsilon_{fd}$$

Extracted this equation

$$k_m(Exp) = \frac{\epsilon_{fe}}{\epsilon_{fd}} \begin{cases} \epsilon_{fe} \text{ taken from experimental test} \\ \epsilon_{fd} \text{ determine by } 0.9\epsilon_{fu} \end{cases}$$

Table. 4: Comparison between experiment and theoretical for determine of K_m (bond-debendedcoffection)

Slab labels	$\epsilon_{fe(Exp)}$	$K_m(Exp)$	$K_m(ACI)$	$K_m(Inhancing)$	$P_{Exp}(KN)$	$P_{ACI}(KN)$	P_{Exp}/P_{ACI}
S1	-	-	-	-	84	83.3	1.01
S2	0.0109	0.72	0.87	0.87	95	95.3	1.01
S3	0.0065	0.34	0.77	0.43	102	102.6	0.99
S4	0.01428	0.74	0.75	0.75	94	94	1.00
S5	0.00528	0.33	0.72	0.37	97	96.7	1.003
S6	0.01389	0.578	0.58	0.58	95	94.9	1.001
S7	0.00728	0.3	0.54	0.29	98	97.9	1.001
S8	0.0066	0.53	0.54	0.54	100	101	0.99
S9	0.0034	0.269	0.27	0.267	88	107	0.82
S10	-	-	-	-	84	90	0.93
S11	0.01392	0.579	0.58	0.58	96	97	0.99
S12	0.00822	0.34	0.54	0.29	107	107.6	0.99

As can be seen from Table 4, the predicted capacities of strengthened slabs with carbon, glass and basalt sheet the onset of yielding of the steel closely matched the measured values with an average of 1% deviation from the experimental results. The predicted capacity of strengthened slabs with carbon laminate by two layers was not closely matched, which the measured value was 18% deviation from the experimental results. The number of plies and thickness of the carbon laminate/sheet are strongly influences the bond results.

The predicted bond-dependent coefficient (K_m) of strengthened slabs with 1 layer from carbon, glass and basalt sheet was closely matched the measured (K_m) from experimental values, but the prediction (K_m) of strengthened slabs with 2 layer wasn't closely matched the measured (K_m) from experimental values. The predicted (K_m) of strengthened slabs with 1,2 layer from enhancing equation was closely matched the measured (K_m) from experimental values

5. CONCLUSION

Based on the results of the current study, the following conclusions could be drawn:

1. The strength and stiffness of the slabs are substantially increased. The ultimate load carrying capacity of the slabs was increased by as much as 130% over their un-strengthened counterpart.
2. The ($A_{\text{fiber}}/A_{\text{steel}}$) ratio is major parameter that affects the performance of strengthened slabs.
3. The debonding failure is prevalent in the tests conducted here. This failure mode is of brittle nature. The average ratio of the strain in the steel at the point of failure was about 2.0 times of the strain in steel at yielding.
4. The prediction capacities of strengthened slabs with carbon, glass and basalt sheet the onset of yielding of the steel closely matched with the measured values from the experimental results.
5. The number of plies and thickness of the carbon laminate/sheet are strongly influences the bond results.
6. The predicted bond-dependent coefficient ($K_{m_{ACI}}$ from ACI equ) of strengthened slabs with 1 layer from carbon, glass and basalt sheet was closely matched the measured (K_m) from experimental values, but the prediction (K_m) of strengthened slabs with 2 layer wasn't closely matched the measured (K_m) from experimental values. The predicted ($K_{m_{\text{enhancing}}}$) of strengthened slabs with 1,2 layer from enhancing equation was closely matched the measured (K_m) from experimental values
7. Further research of the term k_m will likely account not only for stiffness of the laminate/sheet but also for the stiffness of the member to which the laminate is bonded.

Increase the compressive strength of concrete and young modulus of FRP led to late or delay the crack appeared thus increase the cracked load.

Increase the layer number with high young modulus of FRP strengthened was affected in increase the cracked and ultimate load.

Increase the bond-dependent coefficient by increase the young modulus of FRP especially, thus increase the ultimate load. In verse decrease the bond-dependent coefficient by increase number of layers especially when used FRP strips than sheets

REFERENCES

- [1] Aci Committee 440f. Guide For The Design And Construction Of Externally Bonded Frp System For Strengthening Concrete Structures. American Concrete Institute, Detroit, 2000.
- [2] Hassan T, Flexural Performance And Bond Characteristics Of Frp Strengthened Techniques For Concrete Structures, Ph.D. University Of Manitoba, Winnipeg, Manitoba, Canada, 2002; Pp.284.
- [3] Aci 318 (2002). Building Code Requirements For Structural Concrete And Commentary, Aci Committee 318.
- [4] Chan G, Li L, Guo Y, Experimental Study On The Debonding Behaviors Of Cracked Rc Beams Strengthened With Cfrp Sheet, Journal Of Building Structures, Vol. 27, No. 1, 2006, Pp. 99-105.
- [5] Buyukozturk, O. Gunes, O. And Karaca, E. (2004). "Progress On Understanding Debonding Problems In Reinforced Concrete And Steel Members Strengthened Using Frp Composites", Construction And Building Materials, Vol. 18, No. 1, Pp. 9-19.